CALCULATION OF HEAVY-ION FUSION CROSS SECTIONS USING DIFFERENT NUCLEAR POTENTIALS

Aye Myat Wai[1], Nyein Wint Lwin[2]

Abstract

The fusion cross sections and fusion barrier distributions of ^{16}O + $^{148,154}Sm$ systems have been calculated using different types of nuclear potentials. Simple one-dimensional potential model and coupled-channels method have been applied. The calculated results are compared with the experimental data. The calculated fusion cross sections using one-dimensional potential model disagree with the experimental data. The improvements have been made by inclusion of channel coupling effects. The calculated fusion cross sections are also analyzed by calculating the fusion barrier distributions which is sensitive to details structure of the colliding nuclei.

Keywords: different potentials, one-dimensional potential model, coupled-channels method

Introduction

In nuclear physics, heavy-ion is any particle with a mass exceeding that of the helium-4 nucleus (α-particle). Fusion is a process in which two or more nuclei combine to form a compound nucleus. The simplest approach to heavy-ion fusion reactions is to use a one-dimensional potential model. This model deals with only the relative distance between a target and a projectile [Hagino, 1998]. For reactions involving heavy-ions, the fusion cross sections were found to be significantly different from the expectations of such a model, particularly at energies below the barrier where enhancement of several orders of magnitude was observed.

Couplings of the relative motion to nuclear shape deformations and vibrations lead to an enhancement of the sub-barrier fusion cross section in comparison with the predictions of one-dimensional potential model. The couplings produce some interesting features in the barrier distribution for fusion. The fusion barrier distribution is defined as the second derivative of the energy-weighted fusion cross sections with respect the centre-of-mass energy E, that is, $d^2(E\sigma_f)/dE^2$. The barrier distribution has been shown to be sensitive to the data related to the nuclear structure, such as the nuclear shapes, the multiple excitations and the nuclear surface vibrations etc.

In order to make a systematic study of many systems, the choice of the potential is one of the most challenging aspects to compare theory with experimental fusion data both below and above the barrier. The scope of this work is to investigate the fusion cross sections and the corresponding fusion barrier distributions by using different nuclear potentials in the interaction and also take into account the channel coupling effects.

Theoretical framework

A simple estimate of the fusion cross section is obtained by the one dimensional potential model, where one considers the degree of freedom only of the relative motion between the colliding nuclei.

[1.] Dr, Assistant Lecturer, Department of Physics, Monywa University
[2.] Professor, Department of Physics, University of Mandalay

In this model, the fusion cross section for the compound nucleus formation, σ_F, is obtained from the standard formula:

$$\sigma_F(E) = \frac{\pi}{k^2} \sum_l (2l+1)\, P_l(E) \quad , \tag{1}$$

where $P_l(E)$ is the penetrability for the *l*-wave scattering.

The couplings of the relative motion between the colliding nuclei to other degrees of freedom, e.g. their intrinsic excitations, nuclear transfer, can be caused the large enhancement of fusion cross section against predictions of the potential model. They are called channel coupling effects. The coupled-channels calculation is a standard theoretical approach to describe heavy-ion fusion reactions by taking the effects of nuclear intrinsic degrees of freedom into account. The full coupled-channels calculations quickly become very difficult to handle if many physical channels are included. The dimension of the resulting of coupled-channels problem is in general too large if several important intrinsic degrees of freedom exit simultaneously. For this reason, one often introduces the so called the no-Cariolis approximation to avoid these difficulties. In the no-Coriolis approximation, the angular momentum of the relative motion in each channel has been replaced by the total angular momentum J. The coupled-channels equations read

$$\left[-\frac{\hbar^2}{2\mu}\frac{d^2}{dr^2} + \frac{J(J+1)\hbar^2}{2\mu r^2} + V_N(r) + \frac{Z_P Z_T e^2}{r} - E + \varepsilon_n\right]\Psi_n(r) + \sum_m V_{nm}(r)\Psi_m(r) = 0, \tag{2}$$

where Vnm are the matrix elements of the coupling Hamiltonian including the Coulomb and nuclear coupling components. E and ε_n are the bombarding energy in mass center frame and the n-th channel excitation energy, respectively. The coupled equations are solved by using the boundary conditions of the ingoing waves at a radius inside the barrier, and to be matched to appropriate the Coulomb waves at a radius outside the range of the nuclear potential. The minimum position of the Coulomb pocket inside the barrier r_{min}, and the finite distance r_{max} which is the position where both the nuclear and the Coulomb coupling are relatively sufficient small, are adopted by the program. Then the wave functions within r_{min} and beyond r_{max} can be expressed as

$$\Psi_n(r) = T_n \exp\left(-i \int_{r_{min}}^{r} k_n(r')\, dr'\right) r \le r_{min}, \tag{3}$$

$$\Psi_{nm}(r) = C_{nm}\, H_J^{(-)}(k_m r) + D_{nm}\, H_J^{(+)}(k_m r) \quad r \ge r_{max}, \tag{4}$$

with

$$k_n(r) = \sqrt{\frac{2\mu}{\hbar^2}\left(E - \frac{J(J+1)\hbar^2}{2\mu r^2} - V_N(r) - \frac{Z_P Z_T e^2}{r} - \varepsilon_n - V_{nn}(r)\right)} \tag{5}$$

which is the local wave number for the n-th channel and $K_n = K_m$ if r is beyond r_{max} to the infinite. $H_J^{(-)}$ and $H_J^{(+)}$ are the incoming and the outgoing Coulomb functions, respectively.

In order to get the wave functions between r_{min} and r_{max}, the modified Numerov methods have been employed to solve the second order differential equations with setting the conditions at the boundary position r_{min}

$$\Psi_n(r_{min}) = 1, \quad \frac{d}{dr}\Psi_n(r_{min}) = -iK_n(r_{min}). \tag{6}$$

With Eq. (6), the recurrence relation related to wave functions at r_{i+1}, r_i and r_{i-1} are obtained as

$$\Psi^{i+1} = \left(1-\frac{h^2}{12}A^{i+1}\right)^{-1}\left\{\left[\left(\frac{h^2}{\sqrt{12}}A^i+\sqrt{3}\right)^2-1\right]\left(1-\frac{h^2}{12}A^i\right)\Psi^i-\left(1-\frac{h^2}{12}A^{i-1}\right)\Psi^{i-1}\right\}, \tag{7}$$

with

$$A_{nm}(r) = \frac{2\mu}{\hbar^2}\left[\left(\frac{J(J+1)\hbar^2}{2\mu r^2}+V_N(r)+\frac{Z_P Z_T e^2}{r}+\varepsilon_n - E\right)\delta_{n,m} - V_{nm}(r)\right]. \tag{8}$$

And h is the radial step for integrating the equations. By matching the ratio of the wave functions at r_{max}–h to those at r_{max}+h, the coefficients C_{nm} and D_{nm} in Eq. (4) then can be determined. With the above, the solution of the coupled-channels equation can be naturally given by a linear combination of Ψ_{nm}

$$\Psi_m(r) = \sum_n T_n \Psi_{nm}(r). \tag{9}$$

With Eq. (9), the transmission coefficients can be easily obtained. Taking into account all the possible intrinsic states, the inclusive penetrability can be calculated by

$$P^J(E) = \sum_n \frac{k_n(r_{min})}{k}\left|T_n\right|^2. \tag{10}$$

Then, the fusion cross section can be given by

$$\sigma_F(E) = \frac{\pi}{k^2}\sum_J (2J+1)P^J(E). \tag{11}$$

Results and discussion

We investigate the fusion cross sections and fusion barrier distributions by taking the different nuclear potentials in the inter-nuclear interaction. In this work, we use CCFULL code which solves the coupled-channels equations in computing the fusion cross sections, taking the relative motion and the intrinsic degrees of freedom [Hagino *et al*, 1999]. In the original code, Woods-Saxon potential is used as the entrance and coupling potentials. We substitute the original potential in the program with AW, BW, Prox-77 and Prox-88 potentials. These potentials are used as the entrance and coupling potentials in the calculations. We will describe the different nuclear potentials in the following.

A refined version of the Woods-Saxon potential was derived by Broglia and Winther. This refined potential resulted in

$$V_N(r) = -\frac{V_0}{1+\exp[(r-R_0)/a]}, \tag{12}$$

where $V_0 = 16\pi \frac{R_1 R_2}{R_1 + R_2} \gamma a$, a =0.63 fm and $R_0 = R_1 + R_2 + 0.29$. (13)

Here radius R_i has the form $R_i = 1.233 A_i^{1/3} - 0.98 A_i^{-1/3}$ fm $(i = 1, 2)$ and

$$\gamma = \gamma_0 \left[1 - k_s \left(\frac{N_1 - Z_1}{A_1}\right)\left(\frac{N_2 - Z_2}{A_2}\right)\right], \tag{14}$$

where γ_0= 0.95 MeV/fm^2 and k_s= 1.8. We label this potential as BW.

The parameters "*a*" and "R_i" of the above potential were further refined by Winther to a modified form Aage Winther 1995.

$$a = \left[\frac{1}{1.17\left(1 + 0.53\left(A_1^{-\frac{1}{3}} + A_2^{-\frac{1}{3}}\right)\right)}\right] \text{fm}, \tag{15}$$

$$R_i = 1.20 A_i^{1/3} - 0.09 \,\text{fm} \qquad (i = 1, 2). \tag{16}$$

Here, $R_0 = R_1 + R_2$ only. We label this potential as **AW**.

According to the original version of proximity potential 1977, the interaction potential $V_N(r)$ between two surfaces can be written as;

$$V_N(r) = 4\pi \gamma b \bar{R} \Phi\left(\frac{r - C_1 - C_2}{b}\right) \text{MeV}. \tag{17}$$

Where, $C_i = R_i \left[1 - \left(\frac{b}{R_i}\right)^2 + \ldots\right]$, $\bar{R} = \frac{C_1 C_2}{C_1 + C_2}$ and b has the approximate value of 1 fm.

The effective sharp radius, R_i, reads as $R_i = 1.28 A_i^{1/3} - 0.76 + 0.8 A_i^{-1/3}$ fm $(i = 1, 2)$. $\Phi\left(\xi = \frac{r - C_1 - C_2}{b}\right)$ is a universal function which is parameterized with the following form;

$$\Phi(\xi) = -\frac{1}{2}(\xi - 2.54)^2 - 0.0852\,(\xi - 2.54)^3, \text{for } \xi \le 1.2511,$$

$$= -3.437 \exp\left(-\frac{\xi}{0.75}\right), \text{for } \xi \ge 1.2511 \tag{18}$$

and the surface energy coefficient is $\gamma = \gamma_0 \left[1 - k_s \left(\frac{N - Z}{N + Z}\right)^2\right]$. (19)

Where, N and Z are the total number of neutrons and protons. In the present version, γ_0 and k_s were taken to be 0.9517 MeV/fm^2 and 1.7826, respectively [Blocki *et al*, 1977]. We label this potential as **Prox-77**. Later on, using the more refined mass formula due to Möller and Nix, the value of coefficients γ_0 and k_s were modified yielding the values of 1.2496 MeV/fm^2 and 2.3, respectively. We label this potential as **Prox-88**.

We calculate the fusion cross sections for $^{16}O + {}^{148}Sm$ and $^{16}O + {}^{154}Sm$ systems with these different nuclear potentials by using 1-D potential model and coupled-channels method.

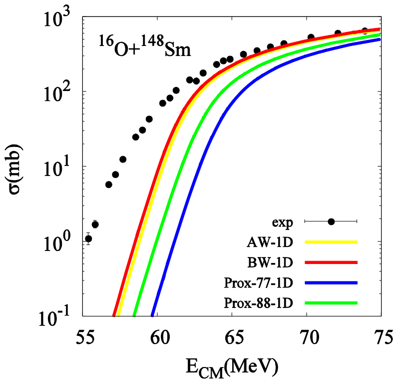

Figure 1 The fusion cross sections for the reaction of ^{16}O + ^{148}Sm system as a function of centre-of-mass energy E_{cm} (MeV). The experimental data are taken from Ref. [Leigh *et al*, 1995].

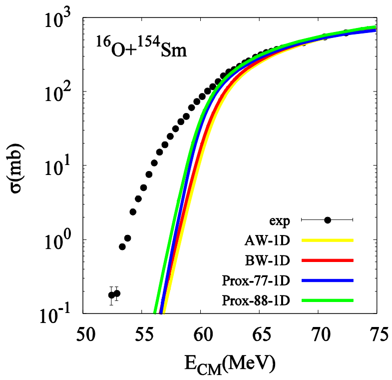

Figure 2 The fusion cross sections for the reaction of ^{16}O + ^{154}Sm system as a function of centre-of-mass energy E_{cm} (MeV). The experimental data are taken from Ref. [Leigh *et al*, 1995].

Fig. 1 and Fig. 2 display the results of fusion cross sections using AW, BW, Prox-77 and Prox-88 potentials for ^{16}O + ^{148}Sm and ^{16}O + ^{154}Sm systems in 1-D potential model. We can see that the results of fusion cross sections for all potentials in one dimensional potential model cannot explain the fusion reactions used in this work. All nuclei considered here are assumed to be spherical in nature; however, deformation as well as orientation of the nuclei (that is channel coupling) can affect the fusion cross sections.

Therefore, we investigate the fusion cross sections and fusion barrier distributions of the same systems using the coupled-channels method. We categorize these systems into two groups having different excitation nature:

(i) Spherical projectile and vibrating target (^{16}O + ^{148}Sm) and

(ii) Spherical projectile and deformed rotating target (^{16}O + ^{154}Sm).

(i) The ^{16}O + ^{148}Sm System

We consider ^{16}O + ^{148}Sm system, ^{148}Sm is considered as vibrating nuclei. In the calculations, we include the quadrupole triple phonon $(2^+)^3$ and octupole triple phonon $(3^-)^3$ states of ^{148}Sm. The excitation energies and the deformation parameters of ^{148}Sm are E_2 = 0.55 MeV, β_2 = 0.182 for 2^+ state and E_3 = 1.16 MeV, β_3 = 0.236 for 3^- state.

Fig. 3 (a) and (b) show the fusion cross sections and the fusion barrier distributions obtained by using AW, BW, Prox-77 and Prox-88 potentials. The results of fusion cross sections with AW and BW potentials slightly underestimate with the experimental data. All potentials can reproduce similar peak character of fusion barrier distributions with the experimental barrier distribution of this system. Prox-77 and Prox-88 potentials give better agreement compared to AW and BW potentials for fusion cross sections as well as the fusion barrier distributions. Interestingly, fusion barrier distribution extracted from the results obtained with Prox-77 potential well reproduces the second peak character in experimental barrier distribution at high energy region (see Fig. 3 (b)).

(ii) The ^{16}O + ^{154}Sm System

In this subsection, the fusion reaction of ^{16}O projectile on ^{154}Sm target has been considered. It is known from the excitation spectra of ^{154}Sm that this nucleus is deformed. Thus, in the calculations it is taken as a well deformed nuclei with deformation parameters β_2 = 0.330, β_4 = 0.050 and excitation energy is E = 0.080 MeV. The fusion cross sections and the corresponding fusion barrier distributions are depicted in Fig. 4 (a) and (b), respectively. The fusion cross sections calculated with Prox-77 and Prox-88 potentials show nearly the same result with the experimental data than that of AW and BW potentials. Concern with fusion barrier distributions, all potentials can reproduce the gross structure of the experimental barrier distribution as shown in Fig. 4 (b). It can be seen that Prox-77 and Prox-88 potentials give better results than AW and BW potentials especially at low energies.

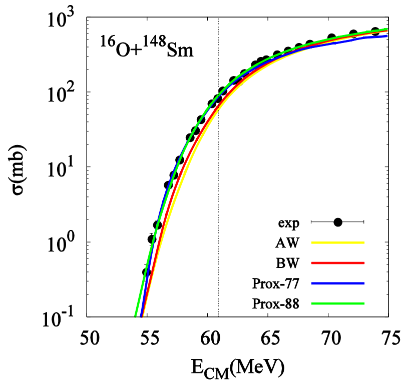

(a)

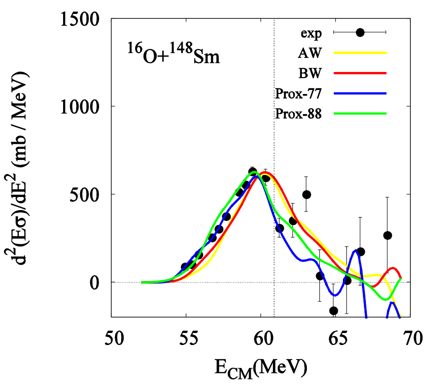

(b)

Figure 3 The comparison of (a) fusion cross sections and (b) the corresponding fusion barrier distributions using different nuclear potentials along with experimental data for ^{16}O + ^{148}Sm system. The vertical line represents the experimental Coulomb barrier height.

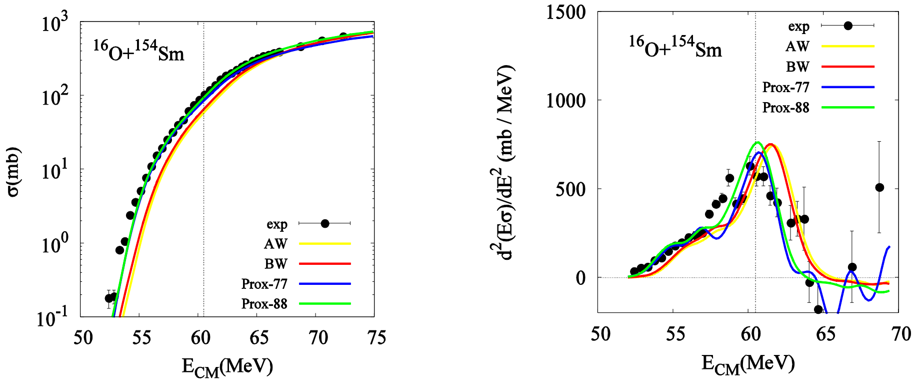

(a) (b)

Figure 4 The comparison of (a) fusion cross sections and (b) the corresponding fusion barrier distributions using different nuclear potentials along with experimental data for ^{16}O + ^{154}Sm system. The vertical line represents the experimental Coulomb barrier height.

Conclusion

We have performed the calculation of fusion cross sections with one dimensional potential model and coupled-channels method for ^{16}O + ^{148}Sm and ^{16}O + ^{154}Sm systems with four different nuclear potentials, namely, AW, BW, Prox-77 and Prox-88. The improvements of fusion cross sections have been made by inclusion of channel coupling effects for all potentials used in this point. According to the calculated fusion cross sections and the corresponding fusion barrier distributions, proximity type potentials give better results than AW and BW potentials and it can be used to make systematic study of heavy-ions fusion reactions.

Acknowledgement

I am grateful thanks to Dr Khin Khin Win, Professor and Head of the Department of Physics, University of Yangon for her kind permission to carry out this work.

I also thank to Professor Dr Shwe Zin Aung, Head of Department of Physics, Monywa University, for her encouragement and permission.

References

Blocki, J. *et al* (1977), "Proximity Forces", Annals of Physics. **105**, pp.427-462.

Hagino, K. (1998), "Multi-Dimensional Quantum Tunneling in Heavy-Ion Fusion Reactions", Tohoku University.

Hagino, K. *et al* (1999), "A Program for Coupled-Channel Calculations with All Order Couplings for Heavy-Ion Fusion Reactions ", vol. **123,** pp.143-152.

Leigh, J. R. *et al* (1995), "Experimental data on HI fusion cross sections", Physical Review, **C 52,** pp.3151.